



Characterization of the actin (*ACT*) family in Rosaceae and role of *PbrACT1* in pear pollen tube growth

Xueying Liu¹ · Hao Zhang¹ · Chao Tang¹ · Shouzheng Lv¹ · Shaoling Zhang¹ · Juyou Wu¹ · Peng Wang¹

Received: 21 October 2023 / Revised: 19 March 2024 / Accepted: 2 April 2024 / Published online: 9 April 2024
© The Author(s), under exclusive licence to Springer-Verlag GmbH Germany, part of Springer Nature 2024

Abstract

The actin (*ACT*) family genes are essential for plant growth and development. However, the evolution and function of the *ACT* family within the Rosaceae species, particularly in pear, remain poorly understood. Here, we identified 41 *ACT* genes across five Rosaceae species based on phylogenetic and structural features that can be categorized into two primary groups: subfamily I (reproductive) and II (vegetative). Evolutionary analysis suggests that purifying selection played a crucial role in the evolution of the *ACT* family in Rosaceae, and whole genome duplication (WGD) and dispersed duplication led to the expansion of *ACT* genes. The pear genome contains twelve *ACT* genes, which can be classified into two groups based on their phylogeny and expression patterns: reproductive (*PbrACT1-5*) and vegetative (*PbrACT6-12*), further validating the reliability of the *ACT* family classification in Rosaceae. Expression analysis of twelve *PbrACT* genes across various pear tissues indicated that five genes from subfamily I (*PbrACT1-5*) were predominantly expressed in pollen tubes, with *PbrACT1* exhibiting the highest level of expression. Knockdown of *PbrACT1* expression in pear pollen tubes significantly diminished F-actin levels, triggered F-actin depolymerization, and resulted in pollen tube growth inhibition, indicating that *PbrACT1* is essential for the formation of the microfilament skeleton during pear pollen tube growth. Overall, this study offers significant insights into the evolution and function of *ACT* genes in Rosaceae and enhances our understanding of *PbrACT* in microfilament formation in pear pollen tubes.

Keywords ACT · Evolution · F-actin · Pear · Pollen tube

Introduction

The actin cytoskeleton, also known as microfilament (MF) or F-actin, is a filamentous polymer built from globular monomers called G-actin. F-actin plays a critical role in plant growth and development. For instance, *Arabidopsis* seedlings treated with the latrunculin (an inhibitor of actin polymerization) caused a significant reduction in cell expansion, resulting in short plants with distorted velvet hairs and smaller than normal lengths of leaves, roots, embryonic

axes, and pollen tubes (Mathur and Hulskamp 2002). Besides, F-actin is also known to be involved in the response to abiotic stresses in plants. For example, treatment of *Arabidopsis* seedlings with 150 mM NaCl induced F-actin polymerization, whereas exposure to 250 mM NaCl led to F-actin degradation. Concurrently, the salt tolerance of seedlings was significantly diminished by treatment with latrunculin A, whereas treatment with phalloidin clearly increased this salinity tolerance (Wang et al. 2010). Similarly, heat stress has been demonstrated to trigger F-actin depolymerization in tobacco BY-2 cells (Malerba et al. 2010). Further, the actin cytoskeleton has been reported to play a vital role in plant immunity (Li and Staiger 2018). The plant microfilament skeleton can resist fungal invasion through dynamic rearrangement (Opalski et al. 2005). In contrast, the penetration efficiency of the fungus is significantly increased when the plants are treated with cytochalasin E, a drug known to disrupt microfilament rearrangements (Kobayashi and Hakuno 2003; Miklis et al. 2007). Moreover, the F-actin plays a critical function in pollen germination, cytoplasmic circulation,

Communicated by A.M. Dandekar.

Xueying Liu and Hao Zhang contributed equally to this work.

✉ Peng Wang
wangpeng@njau.edu.cn

¹ Sanya Institute of Nanjing Agricultural University, State Key Laboratory of Crop Genetics & Germplasm Enhancement and Utilization, Nanjing Agricultural University, Nanjing 210095, Jiangsu, China

and polar growth (Justus et al. 2004; Li et al. 2001; Gibbon et al. 1999; Qu et al. 2014).

Actin is highly conserved and widespread in eukaryotic cells (McElroy et al. 1990; Chang and Huang 2015). In plants, the actin protein is encoded by multiple genes. For example, the *ACT* family of *Arabidopsis* contains eight functionally expressed genes that can be classified into two sub-families based on their phylogenetic and expression profile: vegetative actins (*ACT2*, 7, and 8) are strongly expressed mainly in vegetative organs, and reproductive actins (*ACT1*, 3, 4, 11, and 12) are highly expressed in reproductive tissues (Meagher et al. 1999). The vegetative and reproductive actin are considered functionally redundant due to their strongly conserved amino acid sequences and high identity, such as *ACT1* or *ACT7* driven by the *ACT2* promoter can backfill the *act2-1* mutants (Gilliland et al. 2002). Notably, in *Arabidopsis*, the overexpression of *ACT1*, which is abundantly expressed in vegetative tissues, caused severe alterations in actin cytoskeletal structure and abnormality in plant tissues and cell types, ultimately leading to severe plant dwarfism. However, overexpression of *ACT2* reached similar levels, producing non-significant phenotypic changes (Kandasamy et al. 2007, 2002). The above findings indicated that *ACT* genes of the same type were partially functionally redundant; however, different types of *ACT* genes, besides differing in expression patterns, were not functionally equivalent.

Actin, a key component of the cytoskeleton, is highly abundant in pollen, constituting approximately 2–20% of the total soluble proteins in pollen grains (Xu and Huang 2020). Pollen germination and subsequent growth of pollen tubes are critically dependent on the dynamic actin cytoskeleton (Chang and Huang 2015). For example, pharmacological disruption of F-actin organization and dynamics inhibits both pollen germination and pollen tube growth (Justus et al. 2004; Fang et al. 2018; Gibbon et al. 1999). Additionally, numerous actin-binding proteins (ABPs) participate in the modulation of microfilament dynamics (Ren and Xiang 2007; Zhang et al. 2023). For instance, *Arabidopsis* ADF7 and ADF10 are pollen-specific actin-depolymerizing factors, and their functional loss results in the inhibition of pollen tube growth (Zheng et al. 2013; Jiang et al. 2017). The *Arabidopsis* actin-interacting protein 1 (AIP1) modulates the dynamics and spatial organization of apical microfilaments within pollen tubes, thereby regulating pollen tube growth (Diao et al. 2020). Furthermore, alterations in actin dynamics induce apoptosis or programmed cell death in multiple organisms (Franklin-Tong and Gourlay 2008; Poulter et al. 2010; Thomas et al. 2006). For instance, S-RNase directly interacts with PbrActin1 in pear, leading to the depolymerization of the actin cytoskeleton and facilitating programmed cell death in self-incompatible pollen tubes (Liu et al. 2007; Chen et al. 2018). Similarly, S-RNase interacts with PavAct1 in sweet cherry pollen to disrupt coordinated actin dynamics

in pollen tubes (Matsumoto and Tao 2012). Actin is essential for pollen tube growth; however, the investigation of actin function in Rosaceae is limited.

In this study, we characterized *ACT* genes across five Rosaceae genomes: Pear (*Pyrus bretschneideri*), peach (*Prunus persica*), strawberry (*Fragaria vesca*), apple (*Malus domestica*), and plum (*Prunus mume*). Our analysis encompassed their phylogeny, gene structure, motif identification, and the inference of their expansion history. Additionally, we examined the expression profiles of *PbrACTs* in various tissues and throughout pollen development. Using anti-sense oligodeoxynucleotides (as-ODN) to knock down the *PbrACT1* expression, we found that *PbrACT1* may be required for microfilament skeleton formation and growth in pear pollen tubes. In this work, we conducted a detailed study of *ACT* genes in five Rosaceae species and provided valuable insights for functional studies of ACT proteins in Rosaceae.

Materials and methods

Identification and physicochemical analysis of ACT proteins

Two methods were employed to identify *ACT* family genes across five Rosaceae genomes and obtain their sequences. Firstly, a conserved domain (Pfam: PF00022) search was conducted using the Hidden Markov Model with *E*-values $< 1e^{-5}$ to detect candidate *ACT* members. Subsequently, *Arabidopsis* ACT protein sequences served as queries for BLASTP searches against the genome databases of the five Rosaceae species. Potential *ACT* genes were further validated by consulting the Pfam (<http://pfam.xfam.org>) and SMART (<http://smart.embl-heidelberg.de/>) databases. Finally, 41 *ACT* genes were characterized across the five Rosaceae genomes. The pear genome (v1.0) sequences were sourced from the Pear Genome Project (Wu et al. 2013), while the genome sequences for apple (v1.1), plum (v1.0), peach (v2.1), and strawberry (v4.0) were downloaded from the GDR (<http://www.Rosaceae.org/>). The ExPASy (<http://web.expasy.org/protparam/>) website was utilized to predict the physicochemical properties of ACT proteins (Artimo et al. 2012).

Phylogenetic, gene structure, and motif identification analysis

Phylogenetic trees were constructed using MEGA7.0 with the neighbor-joining method, and their reliability was confirmed through 1000 replicates of bootstrap analysis (Kumar et al. 2016). The gene structure and conserved motifs of *ACT* genes were identified using the GSDS (<http://gsds.gao-lab.com>).

org/) and MEME (<http://meme-suite.org/tools/meme>) websites, respectively (Hu et al. 2015; Bailey et al. 2006). Multiple sequence alignments between ACTs from *Arabidopsis* and Rosaceae were performed using DNAMAN 6.0 with default settings to elucidate sequence features. Consensus sequence logos were generated with WebLogo (<https://weblogo.berkeley.edu/logo.cgi>) (Crooks et al. 2004). Identity of CDS sequences of ACT genes was analyzed by the Clustal Omega tool (<https://www.ebi.ac.uk/Tools/msa/clustalo/>) (Madeira et al. 2022).

Gene duplication modes, syntenic, and Ka/Ks analysis

Initially, syntenic genes were analyzed with methods developed by PGGD (<http://chibba.agtec.uga.edu/duplication/>) (Lee et al. 2013). Subsequently, various duplication modes within the ACT family of five Rosaceae genomes were characterized with MCScanX (Wang et al. 2012). Ultimately, all identified duplication types and syntenic genes were visualized using Circos (Krzywinski et al. 2009). The calculate_Ka_Ks_pipeline was used to generate Ka and Ks values and Ka/Ks ratio (Qiao et al. 2019).

Expression analysis of ACTs in various pear tissues

Different pear tissues (fruits, leaves, stems, roots, styles, and mature pollen) were collected at the fruit experimental field of Nanjing Agricultural University, China. Total RNA was extracted from these tissues using the RNA isolation Kit (Vazyme, China). The RNA samples were then reverse transcribed following the protocol provided with the HiScript® III RT SuperMix for qPCR kits (Vazyme, China). The *PbrACTs*-specific primers were designed by Primer 5.0, and their specificity was verified in the pear genome website (Table S1). Due to the 100% sequence identity in the CDS among *PbrACT9*, *10*, *11*, and *12*, and the 99.21% identity between *PbrACT6* and *7*, which precluded the design of specific primers, co-primers were employed (Table S2). Quantitative real-time PCR (qRT-PCR) was conducted on a LightCycler® 480 II (Roche, Germany) using SYBR qPCR Master Mix (Vazyme, China), with *PbrUBQ* genes as internal control. Expression data were analyzed using the $2^{-\Delta\Delta Ct}$ method.

The antisense oligodeoxynucleotide (as-ODN) assays

The as-ODN assays were conducted as previously described (Chen et al. 2018; Zhang et al. 2024). RNAfold (<https://rna.tbi.univie.ac.at/cgi-bin/RNAWebSuite/RNAfold.cgi>) was utilized to design ODN primers for *PbrACT1* (Table S1). The pollen medium was composed of 0.5 mM $\text{Ca}(\text{NO}_3)_2$, 5

mM 1.5 mM H_3BO_3 , 2-(N-morpholino) ethanesulfonic acid hydrate, and 450 mM sucrose, with the pH adjusted to 6.2 using Tris. Primers with a final concentration of 50 μM ODN were mixed with Lipofectamine 2000 (Thermo Fisher Scientific, USA) and incubated for 15 min. The mixture was then added to the pollen medium that had been pre-incubated for 45 min, followed by further incubation for 2 h. Pollen samples were imaged with a Nikon Eclipse E100 microscope (Tokyo, Japan), and the lengths of at least 50 pollen tubes were measured with Image ProPlus 6.0 software (Media Cybernetics, USA).

F-actin visualization and relative content assay in pollen tubes

F-actin imaging and relative content assays in pear pollen tubes were performed as previously described (Chen et al. 2018). Method for microfilament imaging is summarized as follows: Firstly, pollen tubes were fixed in 4% paraformaldehyde for 1 h following 10 min treatment with 200 μM MES-buffered saline. Subsequently, samples were washed three times with PBS (pH = 6.8). Samples were then stained with 5 μM FITC-phalloidin overnight, followed by three washed with PBS. Finally, samples were anti-fluorescently sealed and observed by LSM800. For F-actin relative content assays, the procedure is as follows: pollen samples were fixed for 1 h and washed three times with PBS. Samples were then stained with 5 μM FITC-phalloidin and 5 μM ethidium bromide (EB) after overnight incubation. Following three washes with PBS, the excess fluorescence was eliminated with methanol. The fluorescence intensity was measured by fluorescence spectrometry. F-actin content was calculated as the ratio of FITC-phalloidin fluorescence (excitation wavelength: 492 nm; emission wavelengths: 514 nm) to EB fluorescence (excitation wavelength: 513 nm; emission wavelengths: 615 nm).

Statistical analysis

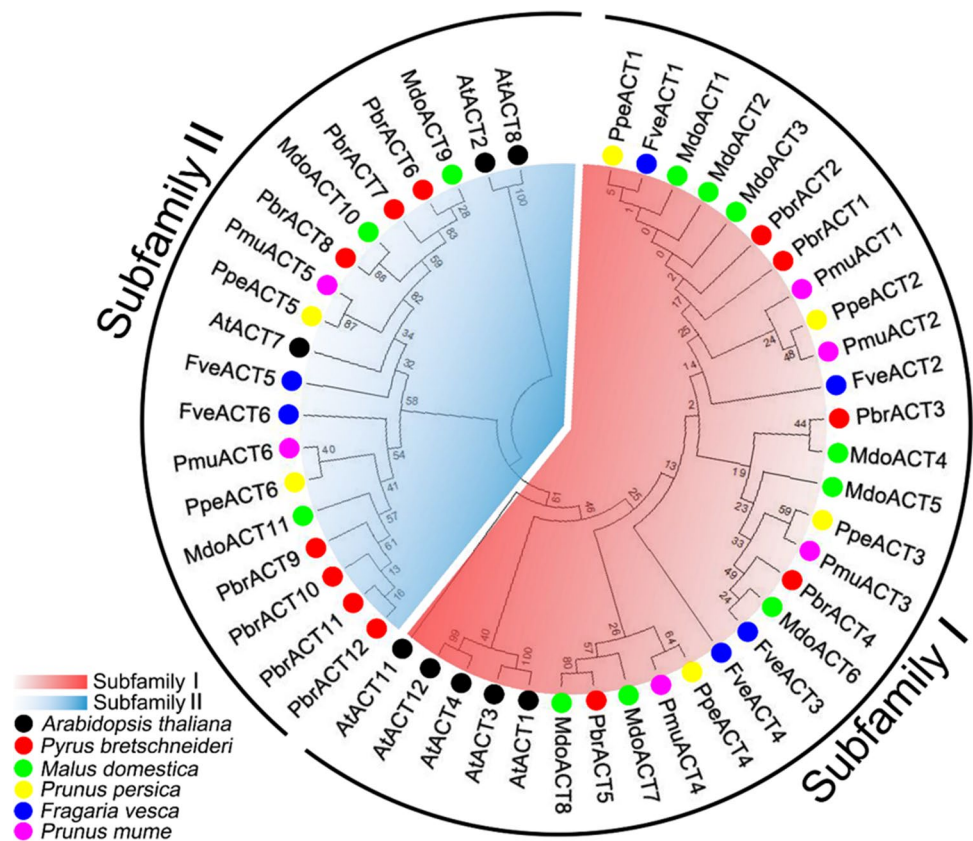
Experiments were conducted with at least three replicates, and data were analyzed using GraphPad Prism 6.01. Statistical differences between the two groups were calculated using Student's *t*-test.

Results

Identification and phylogenetic analysis of ACTs

A total of 41 ACTs were characterized in five Rosaceae species (Fig. 1 and Table S3). Specifically, 12 ACTs were identified in pear (*PbrACTs*), 6 in strawberry (*FveACTs*), 6 in peach (*PpeACTs*), 11 in apple (*MdoACTs*),

Fig. 1 Phylogenetic analysis of the ACT family proteins in Rosaceae and *Arabidopsis*. The phylogenetic tree was constructed based on full-length protein sequences using the neighbor-joining method in MEGA 7.0, with bootstrap analysis assessed through 1000 replicates. The red and blue backgrounds denote the two subfamilies (I and II) of ACT proteins. The species abbreviations and their corresponding colors are as follows: At for *Arabidopsis thaliana* (black), Pbr for *Pyrus bretschneideri* (red), Mdo for *Malus domestica* (green), Ppe for *Prunus persica* (yellow), Fve for *Fragaria vesca* (blue), and Pmu for *Prunus mume* (pink)



and 6 in plum (*PmuACTs*). Notably, the *PbrACTs* exhibited uneven distribution across the pear chromosome, with five genes located on chromosome 15. Additionally, *PbrACT9* (Chr15: 33,484,562–33,486,017), *PbrACT10* (Chr15: 33,428,764–33,430,219), *PbrACT11* (Chr15: 33,284,053–33,285,508), and *PbrACT12* (Chr15: 33,340,016–33,341,471) were found to comprise 377 amino acids (aa), possess an isoelectric point (PI) of 5.31, and a molecular weight (MW) of 41.74 kDa (Table 1, S3). It was further determined that these four genes are identical and are located in neighboring regions of the same chromosome.

Based on the neighbor-joining evolutionary tree, the ACT family members were classified into two subfamilies (subfamily I and II). Notably, subfamily I contains the largest number of ACT genes, with only five ACTs in pear (Fig. 1). Conversely, subfamily II formed a smaller clade, comprising 16 members, including seven ACTs from pear (Fig. 1).

Conserved motif and exon/intron analysis

To investigate the structural diversity of ACT genes in Rosaceae, an exon/intron analysis of the gene sequences was performed. The results indicated that most ACT genes possess four exons, with the exception of nine apple genes (*MdoACT1/3/5–11*), which contain three exons (Fig. 2a).

MEME website was utilized to characterize conserved motifs within ACT proteins. The analysis predicted five motifs for all ACT proteins, except for *MdoACT1*, *MdoACT3*, and *MdoACT5–11*, which exhibited four motifs (Fig. 2b, Table S4), underscoring the relative conservation of ACT proteins during evolution.

To understand the structural characteristics of ACT proteins, we conducted an identity analysis on the amino acid sequence of ACT proteins in *Arabidopsis* and Rosaceae. Our findings revealed a high degree of conservation in ACT protein sequences, with identity percentages ranging from 91.25 to 100% compared to the amino acid sequence of *Arabidopsis* (Table S5). Similarly, the amino acid sequence identity of ACT proteins within pear, apple, peach, plum, and strawberry exhibited high conservation, with identity percentages ranging from 94.96 to 100%, 94.72 to 100%, 96.02 to 99.2%, 95.76 to 99.2%, and 95.76 to 99.47%, respectively (Table S5). Furthermore, we performed multiple sequence alignments for all ACT proteins under investigation. The alignments demonstrated a striking consistency in the amino acid sites between ACT proteins in Rosaceae and *Arabidopsis*, with the notable exception of the N-terminal region in nine apple proteins (*MdoACT1, 3, 5–11*), which exhibited a deletion of 17 amino acids (Fig. S1).

Table 1 Physicochemical analysis of ACT proteins from five Rosaceae species

Gene name	Protein length (aa)	Molecular weight (Da)	Isoelectric points (PI)	GRAVY	Formula	Instability index	Aliphatic index
PbrACT1	377	41,686.73	5.31	-0.175	C ₁₈₅₀ H ₂₉₁₇ N ₄₉₁ O ₅₆₁ S ₂₁	34.87	84.62
PbrACT2	377	41,702.73	5.31	-0.181	C ₁₈₅₀ H ₂₉₁₇ N ₄₉₁ O ₅₆₂ S ₂₁	35.89	84.35
PbrACT3	377	41,684.71	5.31	-0.169	C ₁₈₄₉ H ₂₉₁₅ N ₄₉₃ O ₅₆₀ S ₂₁	36.12	84.88
PbrACT4	377	41,684.75	5.31	-0.167	C ₁₈₅₁ H ₂₉₁₉ N ₄₉₁ O ₅₆₀ S ₂₁	36.85	85.15
PbrACT5	377	41,750.78	5.31	-0.193	C ₁₈₅₀ H ₂₉₁₇ N ₄₉₁ O ₅₆₃ S ₂₂	35.61	83.05
PbrACT6	377	41,786.77	5.31	-0.189	C ₁₈₅₉ H ₂₉₂₅ N ₄₉₁ O ₅₆₄ S ₁₉	39.97	85.09
PbrACT7	377	41,786.77	5.31	-0.189	C ₁₈₅₉ H ₂₉₂₅ N ₄₉₁ O ₅₆₄ S ₁₉	39.97	85.09
PbrACT8	377	41,756.68	5.31	-0.190	C ₁₈₅₈ H ₂₉₂₃ N ₄₉₁ O ₅₆₅ S ₁₈	40.55	85.60
PbrACT9	377	41,739.79	5.31	-0.172	C ₁₈₅₂ H ₂₉₂₀ N ₄₉₄ O ₅₆₀ S ₂₁	37.88	85.62
PbrACT10	377	41,739.79	5.31	-0.172	C ₁₈₅₂ H ₂₉₂₀ N ₄₉₄ O ₅₆₀ S ₂₁	37.88	85.62
PbrACT11	377	41,739.79	5.31	-0.172	C ₁₈₅₂ H ₂₉₂₀ N ₄₉₄ O ₅₆₀ S ₂₁	37.88	85.62
PbrACT12	377	41,739.79	5.31	-0.172	C ₁₈₅₂ H ₂₉₂₀ N ₄₉₄ O ₅₆₀ S ₂₁	37.88	85.62
MdoACT1	360	39,955.84	5.67	-0.173	C ₁₇₈₀ H ₂₈₀₆ N ₄₇₂ O ₅₃₃ S ₁₉	35.22	85.08
MdoACT2	377	41,700.75	5.31	-0.175	C ₁₈₅₁ H ₂₉₁₉ N ₄₉₁ O ₅₆₁ S ₂₁	35.09	84.62
MdoACT3	360	39,955.84	5.67	-0.173	C ₁₇₈₀ H ₂₈₀₆ N ₄₇₂ O ₅₃₃ S ₁₉	35.22	85.08
MdoACT4	377	41,656.70	5.31	-0.168	C ₁₈₄₉ H ₂₉₁₅ N ₄₉₁ O ₅₆₀ S ₂₁	35.61	84.88
MdoACT5	360	39,939.84	5.67	-0.165	C ₁₇₈₀ H ₂₈₀₆ N ₄₇₂ O ₅₃₂ S ₁₉	35.99	85.64
MdoACT6	360	39,923.85	5.67	-0.158	C ₁₇₈₀ H ₂₈₀₆ N ₄₇₂ O ₅₃₁ S ₁₉	35.99	85.92
MdoACT7	360	40,039.94	5.67	-0.192	C ₁₇₈₂ H ₂₈₀₆ N ₄₇₄ O ₅₃₃ S ₂₀	34.69	83.72
MdoACT8	360	40,005.88	5.67	-0.193	C ₁₇₇₉ H ₂₈₀₄ N ₄₇₂ O ₅₃₅ S ₂₀	35.76	83.44
MdoACT9	360	40,025.86	5.67	-0.181	C ₁₇₈₈ H ₂₈₁₂ N ₄₇₂ O ₅₃₅ S ₁₇	40.44	85.86
MdoACT10	360	39,995.77	5.67	-0.182	C ₁₇₈₇ H ₂₈₁₀ N ₄₇₂ O ₅₃₆ S ₁₆	40.81	86.11
MdoACT11	360	39,992.91	5.67	-0.163	C ₁₇₈₂ H ₂₈₀₉ N ₄₇₅ O ₅₃₁ S ₁₉	37.84	86.42
PpeACT1	377	41,716.75	5.31	-0.181	C ₁₈₅₁ H ₂₉₁₉ N ₄₉₁ O ₅₆₂ S ₂₁	36.12	84.35
PpeACT2	377	41,702.73	5.31	-0.181	C ₁₈₅₀ H ₂₉₁₇ N ₄₉₁ O ₅₆₂ S ₂₁	35.38	84.35
PpeACT3	377	41,640.70	5.31	-0.166	C ₁₈₄₉ H ₂₉₁₅ N ₄₉₁ O ₅₅₉ S ₂₁	34.87	85.15
PpeACT4	377	41,704.76	5.31	-0.180	C ₁₈₄₉ H ₂₉₁₅ N ₄₉₁ O ₅₆₁ S ₂₂	35.38	83.58
PpeACT5	377	41,752.73	5.31	-0.175	C ₁₈₆₀ H ₂₉₂₇ N ₄₉₁ O ₅₆₃ S ₁₈	38.87	86.13
PpeACT6	377	41,725.81	5.31	-0.170	C ₁₈₅₃ H ₂₉₂₂ N ₄₉₂ O ₅₆₀ S ₂₁	36.97	85.62
FveACT1	377	41,730.78	5.31	-0.181	C ₁₈₅₂ H ₂₉₂₁ N ₄₉₁ O ₅₆₂ S ₂₁	35.61	84.35
FveACT2	377	41,702.73	5.31	-0.187	C ₁₈₅₀ H ₂₉₁₇ N ₄₉₁ O ₅₆₂ S ₂₁	35.61	84.08
FveACT3	377	41,698.78	5.31	-0.167	C ₁₈₅₂ H ₂₉₂₁ N ₄₉₁ O ₅₆₀ S ₂₁	36.34	85.15
FveACT4	377	41,684.75	5.31	-0.169	C ₁₈₅₁ H ₂₉₁₉ N ₄₉₁ O ₅₆₀ S ₂₁	35.09	84.88
FveACT5	377	41,651.60	5.23	-0.165	C ₁₈₅₁ H ₂₉₁₆ N ₄₉₀ O ₅₆₃ S ₁₉	38.62	86.39
FveACT6	377	41,757.80	5.31	-0.184	C ₁₈₅₃ H ₂₉₂₂ N ₄₉₂ O ₅₆₂ S ₂₁	37.48	85.09
PmuACT1	377	41,776.87	5.31	-0.181	C ₁₈₅₃ H ₂₉₂₃ N ₄₉₁ O ₅₆₂ S ₂₂	35.33	84.08
PmuACT2	377	41,762.84	5.31	-0.181	C ₁₈₅₂ H ₂₉₂₁ N ₄₉₁ O ₅₆₂ S ₂₂	34.59	84.08
PmuACT3	377	41,730.84	5.31	-0.167	C ₁₈₅₂ H ₂₉₂₁ N ₄₉₁ O ₅₆₀ S ₂₂	34.82	84.88
PmuACT4	377	41,764.87	5.31	-0.179	C ₁₈₅₁ H ₂₉₁₉ N ₄₉₁ O ₅₆₁ S ₂₃	34.59	83.32
PmuACT5	377	41,812.85	5.31	-0.175	C ₁₈₆₂ H ₂₉₃₁ N ₄₉₁ O ₅₆₃ S ₁₉	37.69	85.86
PmuACT6	377	41,755.89	5.31	-0.163	C ₁₈₅₄ H ₂₉₂₄ N ₄₉₂ O ₅₅₉ S ₂₂	36.07	85.62

Physicochemical analysis of ACT proteins

To investigate the function of ACT proteins in Rosaceae, a comprehensive analysis of their physicochemical properties was performed (Table 1). We found that the sequence length of ACT proteins varied from 360 to 377 aa, and most

ACTs contain 377 aa. The PI of all ACT proteins are acidic, suggesting that ACT proteins from the Rosaceae family are rich in acidic amino acids. Additionally, the MW of all ACT proteins ranges from 39.92 to 41.81 kDa (Table 1). The negative and positive scores of the grand average of hydrophobicity (GRAVY) score correspond to hydrophilicity and

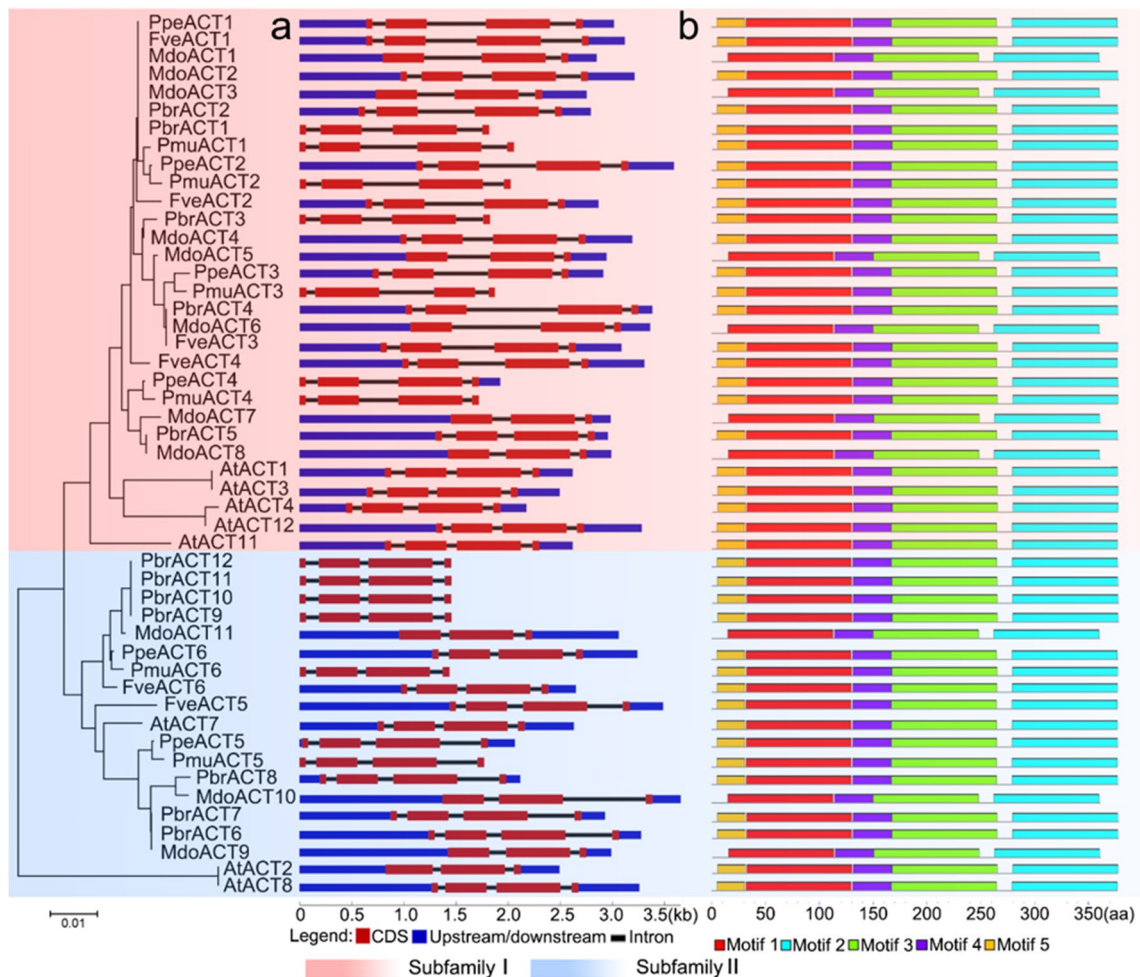


Fig. 2 Exon–intron (a) and conserved motifs (b) analysis of ACT proteins in five Rosaceae species and *Arabidopsis* according to phylogenetic relationships. Neighbor-joining tree was constructed using MEGA 7.0, with bootstrap analysis performed on 1000 replicates and a scale bar representing 0.01 substitutions per site. Exons, introns,

and untranslated regions are represented by red boxes, black lines, and blue boxes, respectively. Five conserved motifs were identified by MEME, with boxes of different colors representing distinct motifs. The red and blue backgrounds denote the two subfamilies (I and II) of ACT proteins in *Arabidopsis* and Rosaceae, respectively.

hydrophobicity, respectively. The findings revealed that all ACT proteins exhibited negative GRAVY score, suggesting that these proteins possess hydrophilic characteristics. Furthermore, the aliphatic indexes of all ACT proteins ranged from 83.05 to 86.42, which indicates that they are thermally stable (Table 1).

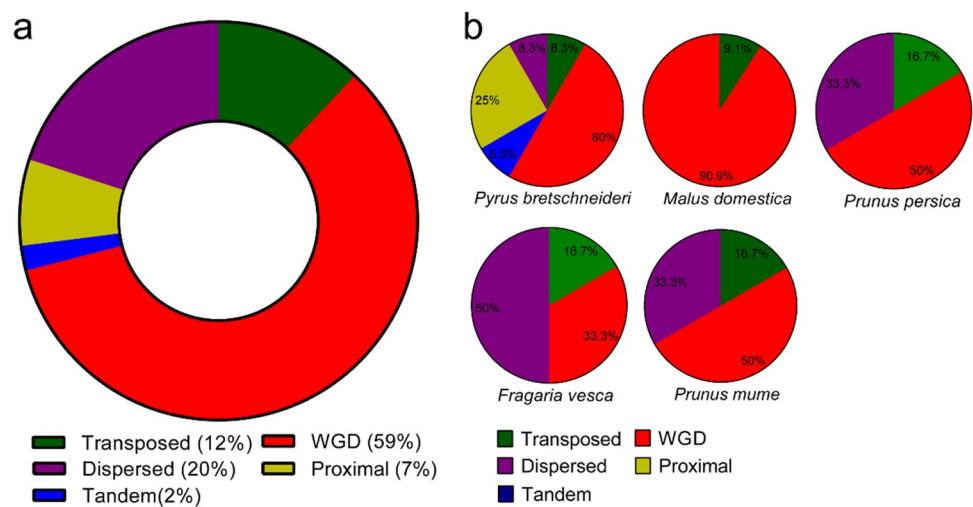
Evolutionary pattern analysis of ACT genes

Several types of gene duplication contribute to the expansion of gene families (Qiao et al. 2019). Our analysis revealed that five duplication types drive the expansion of the ACT family: 59% WGD, 20% dispersal, 12% transposition, 7% proximal, and 2% tandem (Fig. 3a). Notably, WGD was identified in five Rosaceae species. Specifically, 90.9% of ACT genes in apple, 80% in pear, 50% in peach, and 50% in plum were replicated and retained from WGD, while only

33.3% in strawberry (Fig. 3b, Table S6). Furthermore, the percentage of dispersed duplication (DSD) in pear (8.3%), strawberry (50%), peach (33.3%), and plum (33.3%) was assessed (Fig. 3b, Table S6). Transposed duplication was identified at rates of 16.7% in peach, 16.7% in strawberry, 16.7% in plum, and 8.3% in pear (Fig. 3b, Table S6). These findings indicate that WGD significantly affects the expansion of the ACT family in apple, pear, peach, and plum, while DSD plays a key role in the expansion of the strawberry ACT family.

In this study, collinearity maps were generated for each Rosaceae species to investigate the evolution of the ACT genes. The analysis revealed that *PbrACTs* are distributed across seven chromosomes in pear, with eleven syntenic pairs identified (Fig. 4). Among them, eight, six, and seven homozygous gene pairs were detected in *PpeACT*, *FveACT*, and *PmuACT*, respectively (Fig. 4). Furthermore, the

Fig. 3 Statistical analysis of duplication types within the *ACT* family members in Rosaceae species. **a** Statistics of *ACT* genes from different duplication types in Rosaceae genomes. **b** Statistics of *ACT* genes from different duplication types in each Rosaceae genomes. The MCSanX software was utilized to analyze the various duplication patterns within the *ACT* family



distribution of eleven *MdoACTs* was mapped onto eight chromosomes in apple, with twelve syntenic pairs identified (Fig. 4).

To elucidate the selective pressures shaping the evolution of the *ACT* family, we computed K_s values and K_a/K_s ratios for *ACT* gene pairs. The results show that all K_a/K_s ratios are less than 1 (Fig. 5a, Table S7), indicating that the *ACT* family has undergone purifying selection during evolution. Furthermore, K_s values were utilized to infer the evolutionary history of duplication events. The results show that K_s values for all duplicated gene pairs range from 0.0343 to 4.1280 (Table S7). As shown in Fig. 5b and Table S7, the K_s values for gene pairs in pear and apple predominantly corresponded to recent ($K_s \sim 0.15\text{--}0.3$) and ancient ($K_s \sim 1.5\text{--}1.8$) WGD events, whereas peach, plum, and strawberry are mainly associated with ancient WGD. The findings align with previous studies that pear and apple have also experienced recent WGD events compared to strawberry, peach, and plum. Notably, gene pairs with higher K_s values, such as *PbrACT5*-*PbrACT3* ($K_s = 3.96689$), *MdoACT2*-*MdoACT8* ($K_s = 3.91788$), and *MdoACT7*-*MdoACT2* ($K_s = 3.9353$), suggest that they may have originated from more ancient duplication event (Fig. 5b, Table S7).

Expression patterns of *PbrACT* genes

The qRT-PCR method was performed to assess the expression profiles of *PbrACTs* in six pear tissues. The findings revealed that five *PbrACT* genes (*PbrACT1*-5) were strongly expressed in pollen tubes (Fig. 6a). Additionally, the transcriptome data and qRT-PCR results indicated that *PbrACT1* exhibited the highest expression level in pollen tubes compared to other *PbrACT* genes (Fig. 6b, c). Based on previous studies, *Arabidopsis ACT1* and *ACT3* exhibit a preferential accumulation at high levels in mature pollen (An et al. 1996). In this study, the significant expression of *PbrACT1*

in pollen underscores its pivotal role in pear reproductive development.

PbrACT1 controlling pollen tube growth

F-actin is crucial for pollen tube growth (Qu et al. 2014; Zhang et al. 2018; Susaki et al. 2023). To elucidate the role of *PbrACT1*, we utilized the as-ODN assay, a gene knock-down technique, to silence the expression of *PbrACT1* in pear pollen tubes. When the expression of *PbrACT1* was dramatically reduced after as-ODN treatment, pollen tube growth was markedly inhibited (Fig. 7a-c), indicating that *PbrACT1* contributes to pollen tube growth. Subsequently, we observed a significant increase in the rate of F-actin depolymerization in pollen tubes after as-ODN treatment (Fig. 7d, e), along with a significant decrease in F-actin levels (Fig. 7f). These results indicate that the knockdown of *PbrACT1* expression reduces the F-actin content within pollen tubes, thereby inhibiting pollen tube growth. In conclusion, the microfilament skeleton plays a critical role in the growth of pear pollen tubes, and *PbrACT1* contributes importantly to the formation of the microfilament skeleton.

Discussion

F-actin is an important component of the cytoskeleton and plays critical roles in various aspects of plant growth, including root growth, pollen germination and growth, and immune responses (Nishimura et al. 2003; Justus et al. 2004; Li et al. 2001; Li and Staiger 2018; Zepeda et al. 2014; Zhang et al. 2023). *ACT* is essential for F-actin formation, and the *ACT* gene family members have been characterized and analyzed in many species (Meagher et al. 1999; Zhang et al. 2010; Li et al. 2005; McElroy et al. 1990). However, the characterization and functional

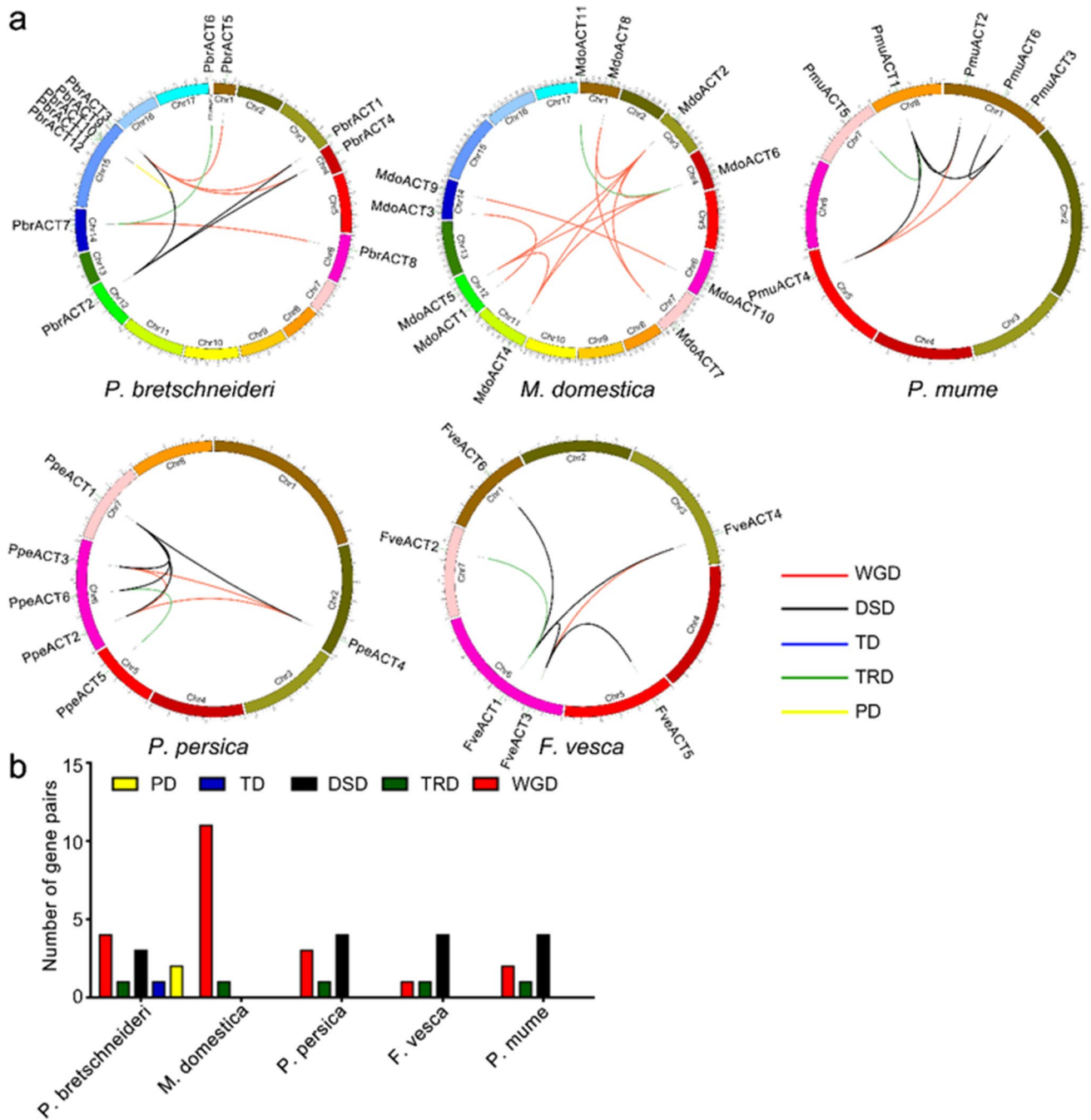


Fig. 4 Intragenomic collinearity and duplication type analysis of the *ACT* family in Rosaceae species. **a** Chromosomal localization and intra-genomic collinearity of *ACT* genes in each Rosaceae genome. Gene pairs connected by lines of different colors represent different duplication types (WGD, whole genome duplication; TD, tandem duplication; TRD, transposed duplication; PD, proximal duplication;

DSD, dispersed duplication). **b** Statistical analysis of various duplication types in five species, including *P. bretschneideri*, *M. domestica*, *P. persica*, *P. mume*, and *F. vesca*. The five colored rectangles represent different types of gene duplication: WGD (red), DSD (black), TD (blue), PD (yellow), and TRD (green). The *Y*-axis indicates the number of duplicated gene pairs

analysis of the *ACT* family in Rosaceae remain limited. In this study, we characterized 41 *ACT* genes within five Rosaceae species (Fig. 1 and Table S3) and investigated that PbrACT1 affects the growth of pear pollen tubes by regulating F-actin levels.

Phylogenetic relationships provided new insights into the evolution and genetic diversity of different gene family members (Smith et al. 2008; Kou et al. 2020). Phylogenetic analysis revealed that *ACT* genes in Rosaceae can be divided into two subgroups (Fig. 1), which classification is

Fig. 5 Ka/Ks ratios (a) and Ks values (b) for duplicated gene pairs within the ACT family in five Rosaceae species, including *P. bretschneideri* (*PbrACTs*), *M. domestica* (*MdoACTs*), *P. persica* (*PpeACTs*), *P. mume* (*PmuACTs*), and *F. vesca* (*FveACTs*). The X-axis represents five different species, while the Y-axis denotes the Ka/Ks ratio or Ks values

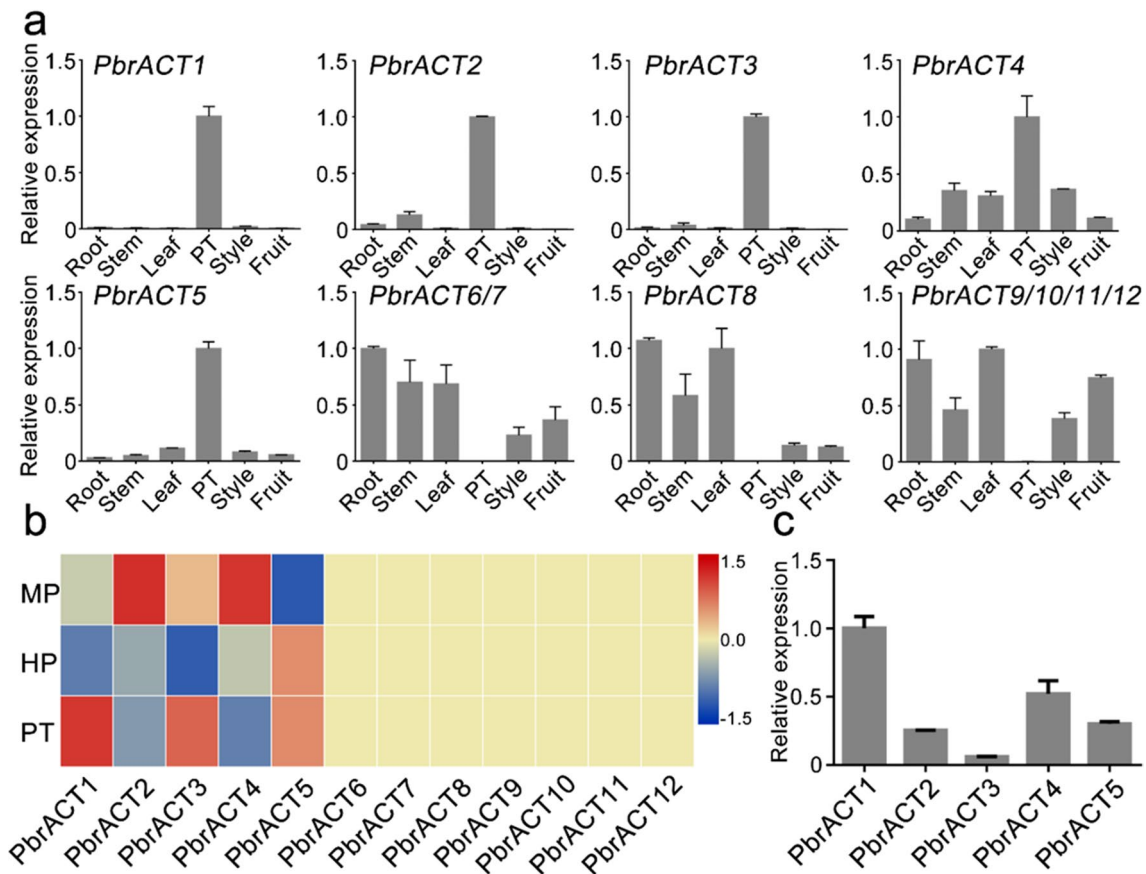
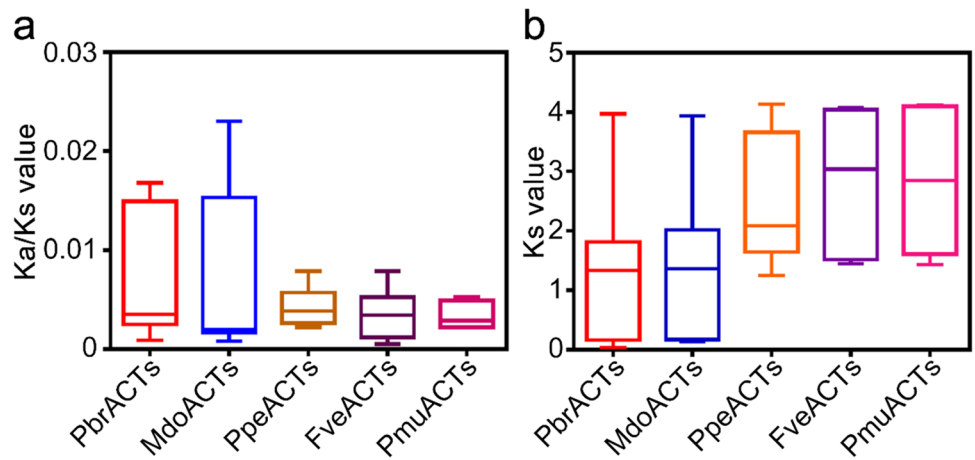


Fig. 6 Expression patterns of twelve *PbrACT* genes. **a** Expression analysis of *PbrACTs* in different pear tissues by qRT-PCR. **b** Expression heatmap of *PbrACT* genes during pollen growth. Red and blue indicate high and low expression, respectively. The three stages of

pear pollen growth include mature pollen grains (MP), hydrated pollen (HP), and pollen tubes growing 6 h after hydration (PT). **c** Expression of five *PbrACTs* in pollen tubes analyzed by qRT-PCR

consistent with that reported on *Arabidopsis* (Kandasamy et al. 2007, 2009). Phylogenetic analysis also demonstrated that *ACTs* with similar gene structures and conserved motifs cluster together (Fig. 2). Furthermore, amino acid sequence alignment and identity analysis indicated

that the Rosaceae *ACT* protein sequences are highly conserved (Fig. S1), with identity ranging from 94.72 to 100% (Table S5). Similarly, the divergence between vegetative and reproductive actins at the amino acid sequence level in *Arabidopsis* ranged from 4 to 7% (Kandasamy et al. 2007).

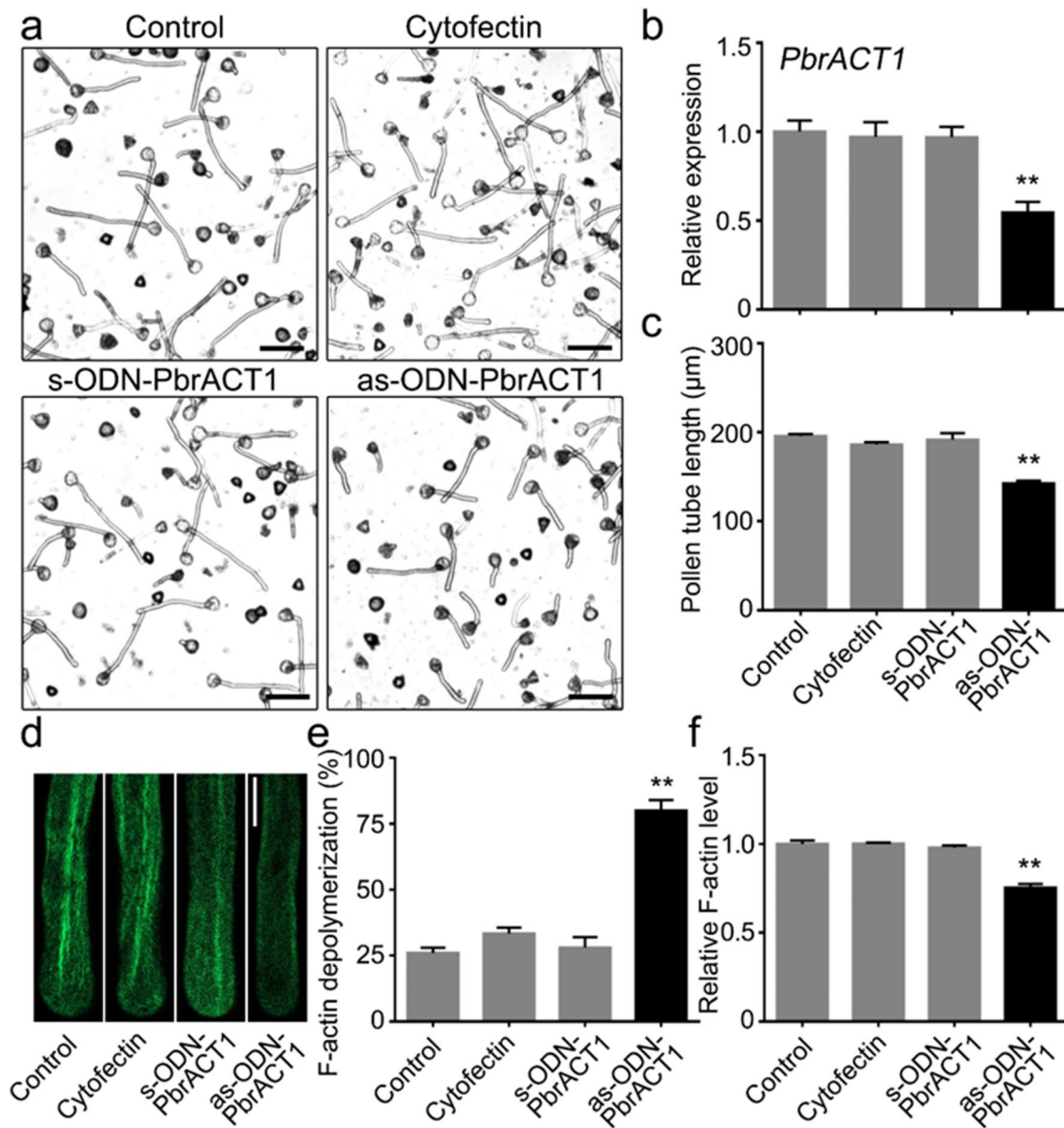


Fig. 7 PbrACT1 promotes pear pollen tube growth. **a** Pollen tube growth was inhibited by as-ODN-PbrACT1 treatment. Bar = 100 μm . **b** Expression level of *PbrACT1* was decreased by as-ODN treatment. **c** Measurement of pollen tube length. **d** Phenotypes of FITC-phalloidin staining in pollen tubes under as-ODN treatment. Bars = 10 μm . **e** Statistics of F-actin depolymerization rate. **f** Measurement of relative F-actin levels. Significant differences ($p < 0.01$) by Student's *t*-test indicated as "**"

din staining in pollen tubes under as-ODN treatment. Bars = 10 μm . **e** Statistics of F-actin depolymerization rate. **f** Measurement of relative F-actin levels. Significant differences ($p < 0.01$) by Student's *t*-test indicated as "**"

The findings suggest that the ACT proteins exhibit a high degree of conservation.

Different patterns of gene duplication within plant genomes play distinct roles in the expansion of gene families (Qiao et al. 2019). Duplication pattern analysis indicates that the expansion of the ACT family in apple, peach, pear, and plum is primarily attributed to WGD, whereas DSD mainly contributes to the expansion of the ACT family in strawberry (Fig. 3 and Table S6). In summary, the expansion of the ACT family in Rosaceae has undergone various duplication types, with WGD and DSD collectively accounting for

approximately 79% of the ACT family genes and serving as the predominant forces in its expansion (Fig. 3a). Previous studies have demonstrated that pear and apple have experienced both recent WGD (30–45 MYA, $K_s \sim 0.15\text{--}0.3$) and ancient WGD (~ 140 MYA, $K_s \sim 1.5\text{--}1.8$) events (Wu et al. 2013; Velasco et al. 2010). However, peach, plum, and strawberry have not undergone a recent WGD event. K_s value analysis revealed that most K_s values in pear and apple are predominantly associated with the two peaks corresponding to WGD events, while the K_s values for peach, plum, and strawberry are mainly distributed around the K_s

values of ancient WGD events (Fig. 5b and Table S7). Consequently, the recent WGD events have contributed to the expansion of the *ACT* family in pear and apple. These findings elucidate why the number of *ACT* genes in pear (12) or apple (11) is nearly double that observed in peach (6), strawberry (6), and plum (6).

Gene expression patterns are often correlated with gene function (Kou et al. 2020). For instance, *Arabidopsis ACT1* and *ACT3* are strongly expressed mainly in pollen, with evidence indicating their distinct and crucial roles in the plant cytoskeleton (An et al. 1996; Vitale et al. 2003). The *PtrACT1* gene is mainly expressed in mature xylem fiber cells, suggesting that it may regulate the formation of mature xylem in the trunk (Zhang et al. 2010). Similarly, the *GhACT1* gene is mainly expressed in fibroblasts and played an essential function in fiber elongation (Li et al. 2005). In this study, the pear genome contains twelve *ACT* genes, which were categorized into two main groups based on their expression patterns: reproductive (*PbrACT1-5*) and vegetative (*PbrACT6-12*) (Fig. 6). Phylogenetic and expression analyses of *PbrACT* genes have further validated the classification of the *ACT* family in Rosaceae (Fig. 1). This study focused on *PbrACT* genes that are pivotal in pear reproduction. Transcriptome data and qRT-PCR results indicated that five *PbrACTs* (*PbrACT1-5*) exhibit low expression levels in various tissues but demonstrate strong expression in pollen tubes, with *PbrACT1* showing the highest expression level (Fig. 6). These findings suggest that PbrACT1 plays an essential role in pear pollen tube growth.

F-actin plays an essential function in plant polar growth (Qu et al. 2020, 2014; Zhang et al. 2018; Kandasamy et al. 2009; Numata et al. 2022; Zhou et al. 2010). For instance, the *Arabidopsis* mutant *act2-1* exhibits reduced root hair length and markedly enlarged root hair bases compared to the wild type (Gilliland et al. 2002). Similarly, the mutant *der1*, which is associated with the microfilament backbone, has been found to display an abnormally enlarged midsection of the root hairs (Ringli et al. 2002). Besides, much pharmacological evidence indicates that disruption of actin structure inhibits pollen germination and pollen tube growth, underscoring the necessity of an intact and dynamic actin cytoskeleton for proper pollen development (Gibbon et al. 1999; Xu and Huang 2020; Gossot and Geitmann 2007). For example, treatment with cytochalasin B, an inhibitor of actin polymerization, inhibits apple and pear pollen germination and pollen tube growth (Fang et al. 2018; Liu et al. 2008). Further, genetic evidence indicates that individual knockdown of the four *ACT* genes (*ACT1*, 3, 4, and 12) did not result in any apparent sterility phenotypes, but simultaneous silencing of these four *ACTs* through RNA interference led to significant reproductive defects (Pawloski et al. 2006). Surprisingly, the loss of *ACT11* function promotes pollen tube growth, possibly as a compensatory response to reduced

F-actin levels (Chang and Huang 2015). Consequently, the F-actin is essential for pollen tube growth. In this study, our findings indicate that PbrACT1 exerts a promotional influence on the growth of pollen tubes. When the expression of *PbrACT1* in pollen tubes was reduced by as-ODN treatment, the growth of pollen tubes was inhibited (Fig. 7a–c). Furthermore, the knockdown of *PbrACT1* expression led to a significant enhancement of F-actin depolymerization and a decrease in F-actin levels in pear pollen tubes (Fig. 7d–f). Consequently, PbrACT1 is critical for F-actin formation during pear pollen tube growth. Overall, our results contribute to a comprehensive understanding of the *ACT* family in Rosaceae, elucidating the pivotal role of PbrACT1 in pollen tube growth and offering a valuable foundation for future research on the functions of other actin proteins within the Rosaceae.

Conclusion

In this study, we characterized 41 *ACT* genes in five Rosaceae genomes, which were divided into two subfamilies. Subsequent evolutionary analyses revealed that purifying selection played a crucial role in the evolution of the *ACT* family in Rosaceae, with whole genome duplication and dispersed duplication leading to the expansion of *ACT* genes. Furthermore, *PbrACT* genes were classified into two major groups based on phylogenetic relationships and expression patterns: reproductive (*PbrACT1-5*) and vegetative (*PbrACT6-12*). Notably, *PbrACT1* exhibits strong expression in pollen tubes and confirms its essential role in F-actin formation during pear pollen tube growth. In summary, these findings contribute to a comprehensive understanding of the Rosaceae *ACT* gene family and offer valuable insights for the functional studies of *ACT* proteins in Rosaceae.

Supplementary Information The online version contains supplementary material available at <https://doi.org/10.1007/s11295-024-01647-9>.

Acknowledgements We thank Dr. Ma Yuehua for technical assistance in using confocal microscopy. Bioinformatic analysis was supported by the High-performance Computing Platform of the Bioinformatics Center of Nanjing Agricultural University.

Funding This work was financially supported by the Jiangsu Agricultural Science and Technology Innovation Fund (CX(22)3044), the open funds of the National Key Laboratory for Germplasm Innovation & Utilization of Horticultural Crops (Horti-KF-2023-05), Ningbo Key Laboratory of Characteristic Horticultural Crops in Quality Adjustment and Resistance Breeding (NBYL2023001), Xinjiang Forestry and Fruit Industry Research System (XJLGCYJSTX05-2024-07), the Project Funded by the Priority Academic Program Development of Jiangsu Higher Education Institutions, Tianshan Talents Program of Xinjiang Uygur Autonomous Region and the Earmarked Fund for China Agriculture Research System (CARS-28).

Data availability The data that support the findings of this study are available from the corresponding author upon reasonable request.

Declarations

Competing interests The authors declare no competing interests.

Data archiving statement All *PbrACT*-related sequences were available from the Pear Genome Project (<http://peargenome.njau.edu.cn>), and the protein sequences of ACT members including apple, peach, strawberry, and plum were downloaded from the GDR (<http://www.rosaceae.org/>) database.

References

- An YQ, Huang S, McDowell JM, McKinney EC, Meagher RB (1996) Conserved expression of the *Arabidopsis* ACT1 and ACT3 actin subclass in organ primordia and mature pollen. *Plant Cell* 8(1):15–30. <https://doi.org/10.1105/tpc.8.1.15>
- Artimo P, Jonnalagedda M, Arnold K, Baratin D, Csardi G, de Castro E, Duvaud S, Flegel V, Fortier A, Gasteiger E, Grosdidier A, Hernandez C, Ioannidis V, Kuznetsov D, Liechti R, Moretti S, Mostaguir K, Redaschi N, Rossier G, Xenarios I, Stockinger H (2012) ExPASy: SIB bioinformatics resource portal. *Nucleic Acids Res* 40:W597–603. <https://doi.org/10.1093/nar/gks400>
- Bailey TL, Williams N, Misleh C, Li WW (2006) MEME: discovering and analyzing DNA and protein sequence motifs. *Nucleic Acids Res* 34:W369–373. <https://doi.org/10.1093/nar/gkl198>
- Chang M, Huang S (2015) *Arabidopsis* ACT11 modifies actin turnover to promote pollen germination and maintain the normal rate of tube growth. *Plant J* 83(3):515–527. <https://doi.org/10.1111/tpj.12910>
- Chen J, Wang P, de Graaf BHH, Zhang H, Jiao H, Tang C, Zhang S, Wu J (2018) Phosphatidic acid counteracts S-RNase signaling in pollen by stabilizing the actin cytoskeleton. *Plant Cell* 30(5):1023–1039. <https://doi.org/10.1105/tpc.18.00021>
- Crooks GE, Hon G, Chandonia JM, Brenner SE (2004) WebLogo: a sequence logo generator. *Genome Res* 14(6):1188–1190. <https://doi.org/10.1101/gr.849004>
- Diao M, Li X, Huang S (2020) *Arabidopsis* AIP1-1 regulates the organization of apical actin filaments by promoting their turnover in pollen tubes. *Sci China Life Sci* 63(2):239–250. <https://doi.org/10.1007/s11427-019-9532-0>
- Fang K, Zhang Q, Yang R, Cao Q, Qin L (2018) Cytochalasin B treatment of apple (*Malus pumila* mill.) pollen tubes alters the cytoplasmic calcium gradient and causes major changes in the cell wall components. *Russ J Plant Physiol* 65(3):384–393. <https://doi.org/10.1134/S1021443718030111>
- Franklin-Tong VE, Gourlay CW (2008) A role for actin in regulating apoptosis/programmed cell death: evidence spanning yeast, plants and animals. *Biochem J* 413(3):389–404. <https://doi.org/10.1042/BJ20080320>
- Gibbon BC, Kovar DR, Staiger CJ (1999) Latrunculin B has differential effects on pollen germination and tube growth. *Plant Cell* 11(12):2349–2363. <https://doi.org/10.1105/tpc.11.12.2349>
- Gilliland LU, Kandasamy MK, Pawloski LC, Meagher RB (2002) Both vegetative and reproductive actin isoforms complement the stunted root hair phenotype of the *Arabidopsis act2-1* mutation. *Plant Physiol* 130(4):2199–2209. <https://doi.org/10.1104/pp.014068>
- Gossot O, Geitmann A (2007) Pollen tube growth: coping with mechanical obstacles involves the cytoskeleton. *Planta* 226(2):405–416. <https://doi.org/10.1007/s00425-007-0491-5>
- Hu B, Jin J, Guo AY, Zhang H, Luo J, Gao G (2015) GSDS 2.0: an upgraded gene feature visualization server. *Bioinformatics* 31(8):1296–1297. <https://doi.org/10.1093/bioinformatics/btu817>
- Jiang Y, Wang J, Xie Y, Chen N, Huang S (2017) ADF10 shapes the overall organization of apical actin filaments by promoting their turnover and ordering in pollen tubes. *J Cell Sci* 130(23):3988–4001. <https://doi.org/10.1242/jcs.207738>
- Justus CD, Anderhag P, Goins JL, Lazzaro MD (2004) Microtubules and microfilaments coordinate to direct a fountain streaming pattern in elongating conifer pollen tube tips. *Planta* 219(1):103–109. <https://doi.org/10.1007/s00425-003-1193-2>
- Kandasamy MK, McKinney EC, Meagher RB (2002) Functional non-equivalency of actin isoforms in *Arabidopsis*. *Mol Biol Cell* 13(1):251–261. <https://doi.org/10.1091/mbc.01-07-0342>
- Kandasamy MK, Burgos-Rivera B, McKinney EC, Ruzicka DR, Meagher RB (2007) Class-specific interaction of profilin and ADF isoforms with actin in the regulation of plant development. *Plant Cell* 19(10):3111–3126. <https://doi.org/10.1105/tpc.107.052621>
- Kandasamy MK, McKinney EC, Meagher RB (2009) A single vegetative actin isoform overexpressed under the control of multiple regulatory sequences is sufficient for normal *Arabidopsis* development. *Plant Cell* 21(3):701–718. <https://doi.org/10.1105/tpc.108.061960>
- Kobayashi I, Hakuno H (2003) Actin-related defense mechanism to reject penetration attempt by a non-pathogen is maintained in tobacco BY-2 cells. *Planta* 217(2):340–345. <https://doi.org/10.1007/s00425-003-1042-3>
- Kou X, Liu Q, Sun Y, Wang P, Zhang S, Wu J (2020) The peptide PbrPSK2 from phytosulfokine family induces reactive oxygen species (ROS) production to regulate pear pollen tube growth. *Front Plant Sci* 11:601993. <https://doi.org/10.3389/fpls.2020.601993>
- Krzywinski M, Schein J, Birol I, Connors J, Gascoyne R, Horsman D, Jones SJ, Marra MA (2009) Circoos: an information aesthetic for comparative genomics. *Genome Res* 19(9):1639–1645. <https://doi.org/10.1101/gr.092759.109>
- Kumar S, Stecher G, Tamura K (2016) MEGA7: molecular evolutionary genetics analysis version 7.0 for bigger datasets. *Mol Biol Evol* 33(7):1870–1874. <https://doi.org/10.1093/molbev/msw054>
- Lee TH, Tang H, Wang X, Paterson AH (2013) PGDD: a database of gene and genome duplication in plants. *Nucleic Acids Res* 41:D1152–1158. <https://doi.org/10.1093/nar/gks1104>
- Li J, Staiger CJ (2018) Understanding cytoskeletal dynamics during the plant immune response. *Annu Rev Phytopathol* 56:513–533. <https://doi.org/10.1146/annurev-phyto-080516-035632>
- Li Y, Zee SY, Liu YM, Huang BQ, Yen LF (2001) Circular F-actin bundles and a G-actin gradient in pollen and pollen tubes of *Lilium davidii*. *Planta* 213(5):722–730. <https://doi.org/10.1007/s004250100543>
- Li XB, Fan XP, Wang XL, Cai L, Yang WC (2005) The cotton ACTIN1 gene is functionally expressed in fibers and participates in fiber elongation. *Plant Cell* 17(3):859–875. <https://doi.org/10.1105/tpc.104.029629>
- Liu ZQ, Xu GH, Zhang SL (2007) *Pyrus pyrifolia* stylar S-RNase induces alterations in the actin cytoskeleton in self-pollen and tubes in vitro. *Protoplasma* 232(1–2):61–67. <https://doi.org/10.1007/s00709-007-0269-4>
- Liu Z, Jiang X, Xu G, Zhang S (2008) Effects of cytochalasin B and phalloidin on *Pyrus pyrifolia* self-incompatible pollen germination and tube growth. *Acta Botan Boreali-Occiden Sin* 28(12):2393–2399
- Madeira F, Pearce M, Tivey ARN, Basutkar P, Lee J, Edbali O, Madhusoodanan N, Kolesnikov A, Lopez R (2022) Search and sequence analysis tools services from EMBL-EBI in 2022. *Nucleic Acids Res* 50(W1):W276–W279. <https://doi.org/10.1093/nar/gkac240>
- Malerba M, Crosti P, Cerana R (2010) Effect of heat stress on actin cytoskeleton and endoplasmic reticulum of tobacco BY-2 cultured

- cells and its inhibition by Co^{2+} . *Protoplasma* 239(1–4):23–30. <https://doi.org/10.1007/s00709-009-0078-z>
- Mathur J, Hulskamp M (2002) Microtubules and microfilaments in cell morphogenesis in higher plants. *Curr Biol* 12(19):R669–676. [https://doi.org/10.1016/s0960-9822\(02\)01164-8](https://doi.org/10.1016/s0960-9822(02)01164-8)
- Matsumoto D, Tao R (2012) Isolation of pollen-expressed actin as a candidate protein interacting with S-RNase in *Prunus avium* L. *J Jpn Soc Hortic Sci* 81(1):41–47. <https://doi.org/10.2503/jjshs1.81.41>
- McElroy D, Rothenberg M, Reece KS, Wu R (1990) Characterization of the rice (*Oryza sativa*) actin gene family. *Plant Mol Biol* 15(2):257–268. <https://doi.org/10.1007/BF00036912>
- Meagher RB, McKinney EC, Vitale AV (1999) The evolution of new structures: clues from plant cytoskeletal genes. *Trends Genet* 15(7):278–284. [https://doi.org/10.1016/s0168-9525\(99\)01759-x](https://doi.org/10.1016/s0168-9525(99)01759-x)
- Miklis M, Consonni C, Bhat R, Lipka V, Schulze-Lefert P, Panstruga R (2007) Barley MLO modulates actin-dependent and actin-independent antifungal defense pathways at the cell periphery. *Plant Physiol* 144(2):1132–1143. <https://doi.org/10.1104/pp.107.098897>
- Nishimura T, Yokota E, Wada T, Shimmen T, Okada K (2003) An *Arabidopsis* ACT2 dominant-negative mutation, which disturbs F-actin polymerization, reveals its distinctive function in root development. *Plant Cell Physiol* 44(11):1131–1140. <https://doi.org/10.1093/pcp/pcg158>
- Numata T, Sugita K, Ahamed Rahman A, Rahman A (2022) Actin isovariant ACT7 controls root meristem development in *Arabidopsis* through modulating auxin and ethylene responses. *J Exp Bot* 73(18):6255–6271. <https://doi.org/10.1093/jxb/erac280>
- Opalski K, Schultheiss H, Kogel K, Hüchelhoven R (2005) The receptor-like MLO protein and the RAC/ROP family G-protein RACB modulate actin reorganization in barley attacked by the biotrophic powdery mildew fungus *Blumeria graminis* f.sp. *hordei*. *Plant J* 41(2):291–303. <https://doi.org/10.1111/j.1365-313X.2004.02292.x>
- Pawloski L, Kandasamy M, Meagher R (2006) The late pollen actins are essential for normal male and female development in *Arabidopsis*. *Plant Mol Biol* 62(6):881–896. <https://doi.org/10.1007/s11103-006-9063-5>
- Poulter NS, Staiger CJ, Rappoport JZ, Franklin-Tong VE (2010) Actin-binding proteins implicated in the formation of the punctate actin foci stimulated by the self-incompatibility response in *Papaver*. *Plant Physiol* 152(3):1274–1283. <https://doi.org/10.1104/pp.109.152066>
- Qiao X, Li Q, Yin H, Qi K, Li L, Wang R, Zhang S, Paterson AH (2019) Gene duplication and evolution in recurring polyploidization-diploidization cycles in plants. *Genome Biol* 20(1):38. <https://doi.org/10.1186/s13059-019-1650-2>
- Qu X, Jiang Y, Chang M, Liu X, Zhang R, Huang S (2014) Organization and regulation of the actin cytoskeleton in the pollen tube. *Front Plant Sci* 5:786. <https://doi.org/10.3389/fpls.2014.00786>
- Qu X, Wang Q, Wang H, Huang S (2020) Visualization of actin organization and quantification in fixed *Arabidopsis* pollen grains and tubes. *Bio Protoc* 10(1):e3509. <https://doi.org/10.21769/BioProtoc.3509>
- Ren H, Xiang Y (2007) The function of actin-binding proteins in pollen tube growth. *Protoplasma* 230:171–182. <https://doi.org/10.1007/s00709-006-0231-x>
- Ringli C, Baumberger N, Diet A, Frey B, Keller B (2002) ACTIN2 is essential for bulge site selection and tip growth during root hair development of *Arabidopsis*. *Plant Physiol* 129(4):1464–1472. <https://doi.org/10.1104/pp.005777>
- Smith LL, Fessler JL, Alfaro ME, Streebman JT, Westneat MW (2008) Phylogenetic relationships and the evolution of regulatory gene sequences in the parrotfishes. *Mol Phylogenet Evol* 49(1):136–152. <https://doi.org/10.1016/j.ympev.2008.06.008>
- Susaki D, Izumi R, Oi T, Takeuchi H, Shin JM, Sugi N, Kinoshita T, Higashiyama T, Kawashima T, Maruyama D (2023) F-actin regulates the polarized secretion of pollen tube attractants in *Arabidopsis* synergid cells. *Plant Cell* 35(4):1222–1240. <https://doi.org/10.1093/plcell/koac371>
- Thomas SG, Huang S, Li S, Staiger CJ, Franklin-Tong VE (2006) Actin depolymerization is sufficient to induce programmed cell death in self-incompatible pollen. *J Cell Biol* 174(2):221–229. <https://doi.org/10.1083/jcb.200604011>
- Velasco R, Zharkikh A, Affourtit J, Dhingra A, Cestaro A, Kalyanaraman A, Fontana P, Bhatnagar SK, Troggio M, Pruss D, Salvi S, Pindo M, Baldi P, Castelletti S, Cavaiuolo M, Coppola G, Costa F, Cova V, Dal Ri A, Goremykin V, Komjanc M, Longhi S, Magnago P, Malacarne G, Malnoy M, Micheletti D, Moretto M, Perazzolli M, Si-Ammour A, Vezzulli S, Zini E, Eldredge G, Fitzgerald LM, Gutin N, Lanchbury J, Macalma T, Mitchell JT, Reid J, Wardell B, Kodira C, Chen Z, Desany B, Niazi F, Palmer M, Koepke T, Jiwan D, Schaeffer S, Krishnan V, Wu C, Chu VT, King ST, Vick J, Tao Q, Mraz A, Stormo A, Stormo K, Bogden R, Ederle D, Stella A, Vecchietti A, Kater MM, Masiero S, Lasserre P, Lespinasse Y, Allan AC, Bus V, Chagne D, Crowhurst RN, Gleave AP, Lavezzo E, Fawcett JA, Proost S, Rouze P, Sterck L, Toppo S, Lazzari B, Hellens RP, Durel CE, Gutin A, Bumgarner RE, Gardiner SE, Skolnick M, Egholm M, Van de Peer Y, Salamini F, Viola R (2010) The genome of the domesticated apple (*Malus x domestica* Borkh.). *Nat Genet* 42(10):833–839. <https://doi.org/10.1038/ng.654>
- Vitale A, Wu RJ, Cheng Z, Meagher RB (2003) Multiple conserved 5' elements are required for high-level pollen expression of the *Arabidopsis* reproductive actin ACT1. *Plant Mol Biol* 52(6):1135–1151. <https://doi.org/10.1023/b:plan.0000004309.06973.16>
- Wang C, Zhang L, Yuan M, Ge Y, Liu Y, Fan J, Ruan Y, Cui Z, Tong S, Zhang S (2010) The microfilament cytoskeleton plays a vital role in salt and osmotic stress tolerance in *Arabidopsis*. *Plant Biol* 12(1):70–78. <https://doi.org/10.1111/j.1438-8677.2009.00201.x>
- Wang Y, Tang H, Debarry J, Tan X, Li J, Wang X, Lee T, Jin H, Marler B, Guo H, Kissinger J, Paterson A (2012) MCScanX: a toolkit for detection and evolutionary analysis of gene synteny and collinearity. *Nucleic Acids Res* 40(7):e49. <https://doi.org/10.1093/nar/gkr1293>
- Wu J, Wang Z, Shi Z, Zhang S, Ming R, Zhu S, Khan MA, Tao S, Korban SS, Wang H, Chen NJ, Nishio T, Xu X, Cong L, Qi K, Huang X, Wang Y, Zhao X, Wu J, Deng C, Gou C, Zhou W, Yin H, Qin G, Sha Y, Tao Y, Chen H, Yang Y, Song Y, Zhan D, Wang J, Li L, Dai M, Gu C, Wang Y, Shi D, Wang X, Zhang H, Zeng L, Zheng D, Wang C, Chen M, Wang G, Xie L, Sovero V, Sha S, Huang W, Zhang S, Zhang M, Sun J, Xu L, Li Y, Liu X, Li Q, Shen J, Wang J, Paull RE, Bennetzen JL, Wang J, Zhang S (2013) The genome of the pear (*Pyrus bretschneideri* Rehd). *Genome Res* 23(2):396–408. <https://doi.org/10.1101/gr.144311.112>
- Xu Y, Huang S (2020) Control of the actin cytoskeleton within apical and subapical regions of pollen tubes. *Front Cell Dev Biol* 8:614821. <https://doi.org/10.3389/fcell.2020.614821>
- Zepeda I, Sanchez-Lopez R, Kunkel JG, Banuelos LA, Hernandez-Barrera A, Sanchez F, Quinto C, Cardenas L (2014) Visualization of highly dynamic F-actin plus ends in growing *Phaseolus vulgaris* root hair cells and their responses to *Rhizobium etli* nod factors. *Plant Cell Physiol* 55(3):580–592. <https://doi.org/10.1093/pcp/pct202>
- Zhang D, Du Q, Xu B, Zhang Z, Li B (2010) The actin multigene family in *Populus*: organization, expression and phylogenetic analysis. *Mol Genet Genomics* 284(2):105–119. <https://doi.org/10.1007/s00438-010-0552-5>
- Zhang R, Xu Y, Yi R, Shen J, Huang S (2023) Actin cytoskeleton in the control of vesicle transport, cytoplasmic organization, and

- pollen tube tip growth. *Plant Physiol* 193(1):9–25. <https://doi.org/10.1093/plphys/kiad203>
- Zhang H, Liu X, Tang C, Lv S, Zhang S, Wu J, Wang P (2024) PBRbohH/J mediates ROS generation to regulate the growth of pollen tube in pear. *Plant Physiol Bioch* 207:108342. <https://doi.org/10.1016/j.plaphy.2024.108342>
- Zhang S, Wang C, Xie M, Liu J, Kong Z, Su H (2018) Actin bundles in the pollen tube. *Int J Mol Sci* 19 (12). <https://doi.org/10.3390/ijms19123710>
- Zheng Y, Xie Y, Jiang Y, Qu X, Huang S (2013) *Arabidopsis* actin-depolymerizing factor7 severs actin filaments and regulates actin cable turnover to promote normal pollen tube growth. *Plant Cell* 25(9):3405–3423. <https://doi.org/10.1105/tpc.113.117820>
- Zhou Y, Yang Z, Guo G, Guo Y (2010) Microfilament dynamics is required for root growth under alkaline stress in *Arabidopsis*. *J Integr Plant Biol* 52(11):952–958. <https://doi.org/10.1111/j.1744-7909.2010.00981.x>

Publisher's Note Springer Nature remains neutral with regard to jurisdictional claims in published maps and institutional affiliations.

Springer Nature or its licensor (e.g. a society or other partner) holds exclusive rights to this article under a publishing agreement with the author(s) or other rightsholder(s); author self-archiving of the accepted manuscript version of this article is solely governed by the terms of such publishing agreement and applicable law.